# Indonesian Physical Review

Volume 09 Issue 03, September 2026

P-ISSN: 2615-1278, E-ISSN: 2614-7904

# Synthesis of Nanosilica from Tukad Telaga Waja Sand Using the Coprecipitation Method with NaOH Variations

**Ni Kadek Cinta Eka Putri Jayanti[1*], Ida Bagus Putu Mardana[1*], Putu Yasa[1*], I Komang Restu Widi Artha[2*]**

[1] *Department of Physics and Science Education, Faculty of Mathematics and Natural Science, Ganesha University of Education, Indonesia*

[2] *Physics Department, Bandung Institute of Technology, Indonesia*

*Corresponding Authors E-mail: cinta@student.undiksha.ac.id, putu.mardana@undiksha.ac.id, pt.yasa@undiksha.ac.id, 20225001@mahasiswa.itb.ac.id*

**Article Info**

***Article info:***

*Received: 02-04-2026*

*Revised: 21-07-2026*

*Accepted: 24-07-2026*

***Keywords:***

*Volcanic Sand; Coprecipitation Method; Nanosilica; NaOH Variation*

***How To Cite:***

*N. K. C. E. P. Jayanti, I. B. P. Mardana, P. Yasa, and I. K. R. W. Artha, "Synthesis of Nanosilica from Tukad Telaga Waja Sand Using the Coprecipitation Method with NaOH Variations," Indonesian Physical Review, vol. 9, no. 3, pp. 549–568, 2026.*

***DOI:***

*https://doi.org/10.29303/ipr.v9i3.676.*

**Abstract**

*Volcanic sand is a potential natural silica source for the synthesis of high-value nanosilica materials. This study investigated the effect of NaOH concentration on the chemical composition, crystallinity, and morphology of nanosilica synthesized from Tukad Telaga Waja volcanic sand using the coprecipitation method. The utilization of Tukad Telaga Waja volcanic sand as a local precursor for nanosilica synthesis remains rarely reported, particularly regarding the influence of alkaline extraction conditions on nanosilica formation. The synthesis was carried out at 6 M, 7 M, and 8 M NaOH, followed by acid precipitation. The synthesized materials were characterized using X-ray fluorescence (XRF), X-ray diffraction (XRD), and Scanning Electron Microscopy (SEM). The XRF results showed that increasing NaOH concentration improved the $SiO_2$ purity of the synthesized nanosilica from 96.4 wt% at 6 M to 98.9 wt% at 8 M, indicating enhanced silica extraction during alkaline dissolution. XRD analysis confirmed that all samples exhibited an amorphous structure, with a broad diffraction hump centered at approximately 23 ° in the 2θ range of 20°–30 °. SEM observations revealed irregular granular morphology with agglomerated particle structures. Image analysis of the SEM micrographs using a log-normal distribution approach indicated that the estimated SEM particle domain size decreased from 8.30 nm to 6.05 nm with increasing NaOH concentration. Among the investigated conditions, 8 M NaOH produced nanosilica with the highest purity and the smallest estimated SEM particle domain size. These findings indicate that NaOH concentration plays an important role in controlling silica extraction and the resulting characteristics of amorphous nanosilica synthesized from local volcanic sand. The synthesized nanosilica may be further explored for applications requiring high surface area, such as adsorbents, catalyst supports, and functional composite fillers.*

## Introduction

Silica ($SiO_2$) is one of the primary macromolecular materials found in the Earth's crust. Nanoparticle-sized silica (1-100 nm) is known to have better activity compared to microparticle-sized silica [1]. At the nanometer scale, silica is known to have a high surface area, thermal stability, and silanol groups, which make it useful for various applications, such as adsorption and surface modification, due to its high adsorption capacity and surface modification capabilities [2,3,4]. In recent years, demand for nanosilica has increased significantly, driven by the rapid development of functional materials and nanotechnology-based industries. According to a 2025 Grand View Research report, the global specialty silica market is projected to grow from USD 9.1 billion in 2026 to USD 14.6 billion by 2033, driven by rising demand for high-purity silica for various industrial applications. However, commercially available nanosilica is generally produced using synthetic precursors and relatively expensive processes, thereby encouraging the exploration of alternative silica sources derived from natural materials that are more economical, sustainable, and environmentally friendly [5,6].

Bali Island has two main volcanoes, namely Mount Batur and Mount Agung, with Mount Agung being the highest and most active. Its periodic eruptions produce lahar deposits and pyroclastic materials that are transported through river systems, including Tukad Telaga Waja [7]. This river carries volcanic materials in the form of dark gray to black sand, which is abundant and widely used as construction material, and is one of the major sand mining resources in the Karangasem region [8]. However, the volcanic sand from this area is generally utilized only as a low-value construction material despite its potential silica content. Based on its physical characteristics, such as fine texture, low density, and non-magnetic properties, volcanic sand from Tukad Telaga Waja is expected to contain a significant amount of silica, particularly in amorphous or semi-crystalline forms, making it a promising precursor for high-value nanosilica synthesis [9]. Therefore, utilizing this local volcanic resource as a nanosilica precursor may add economic value while supporting the development of sustainable, high-value functional materials derived from local natural resources.

Volcanic materials are generally formed through fragmentation, weathering, sedimentation, and rapid cooling during volcanic eruptions, resulting in silica-rich materials that retain impurities such as $Al_2O_3$, $Fe_2O_3$, CaO, and MgO [10,11]. The formation of silica-rich volcanic deposits is commonly associated with felsic volcanic materials and geological sedimentation processes that contribute to the accumulation of silica-bearing sands with high industrial potential. Several previous studies have demonstrated the potential of volcanic materials as silica precursors for nanosilica synthesis. Astari et al. reported that volcanic sand from Mount Kelud contains approximately 45–55% $SiO_2$ before purification [11]. In addition, Yogantari and Sulistyani reported that volcanic sands from Mount Merapi, particularly those collected from the Gendol, Kuning, and Opak rivers, contain nearly 50% silica, with albite as the dominant component [12]. Artha et al. also successfully synthesized amorphous nanosilica from Mount Batur volcanic rock in Bali, with a $SiO_2$ purity of 94.9%, using the coprecipitation method [13]. Furthermore, Utari et al. reported that silica gel was successfully synthesized from Mount Agung volcanic ash, yielding 15.05 wt% [9]. Hasanah et al. also reported that volcanic ash could produce nanosilica with $SiO_2$ purity of up to 99.1% via chemical extraction and coprecipitation [14]. These findings indicate that volcanic materials from various regions of Indonesia have significant potential as natural silica precursors for the production of high-purity nanosilica.

The coprecipitation method is one of the most widely employed methods for nanosilica synthesis due to its simple process, relatively low operating temperature, and better energy efficiency compared to alkali fusion methods [15]. In this method, silica is first dissolved in an alkaline solution to form soluble sodium silicate ($Na_2SiO_3$), then acidified to produce amorphous silica particles. The NaOH concentration plays an important role in controlling silica dissolution and nanoparticle formation, as hydroxide ions ($OH^-$) facilitate the cleavage of Si–O–Si bonds within the silica network during the extraction process [16]. Increasing NaOH concentration generally improves silica extraction efficiency and silica purity by promoting the formation of soluble silicate species [17,18,19]. However, excessively high NaOH concentration may increase solution viscosity and interparticle interactions, thereby increasing particle collision frequency and promoting agglomeration, thereby reducing the quality of the synthesized nanosilica [20,21].

Several previous studies have investigated the effect of NaOH concentration on nanosilica synthesis via coprecipitation. Meilani et al. reported that increasing NaOH concentration from 2.5 M to 7.5 M in $SiO_2$ synthesis from red mud increased the $SiO_2$ purity from 27.2% to 47.6% [18]. Owoeye et al. also successfully synthesized nanosilica from glass powder using NaOH concentrations of 3 M, 4 M, and 5 M, with the highest purity of 97.21% obtained at 5 M [22]. In addition, Siswanto et al. demonstrated that increasing NaOH concentration from 6 M to 8 M in $SiO_2$ synthesis from Bangka Belitung beach sand and Lumajang River sand improved the $SiO_2$ purity up to 96.7% at 8 M [23]. Meanwhile, Ramadhan et al. found that the optimum $SiO_2$ purity of 96.1% was achieved at 9 M NaOH during the synthesis of $SiO_2$ from Bancar beach sand; however, increasing the NaOH concentration to 11 M reduced silica purity due to increased particle agglomeration during the precipitation process [24]. Therefore, the NaOH concentration range of 6 M, 7 M, and 8 M was selected in this study because previous studies demonstrated that this concentration range effectively enhanced silica extraction and purity while minimizing excessive agglomeration in silica-rich sand materials. In particular, Siswanto et al. successfully applied the same NaOH concentration range to silica synthesis from river-derived sand materials, which are considered comparable to the volcanic sand deposits transported through the Tukad Telaga Waja river system of Mount Agung.

Although several studies have reported the synthesis of nanosilica from beach sand, volcanic ash, and other natural silica sources in Indonesia, the influence of NaOH concentration on the purity, amorphous structure, and morphology of nanosilica synthesized specifically from Tukad Telaga Waja volcanic sand remains insufficiently investigated. This study, therefore, addresses this research gap by utilizing Tukad Telaga Waja volcanic sand as a local silica precursor and systematically evaluating the effect of NaOH concentrations of 6 M, 7 M, and 8 M on the purity, amorphous structure, and morphology of the synthesized nanosilica using XRF, XRD, and SEM characterization. Accordingly, this study aims to synthesize and characterize nanosilica derived from Tukad Telaga Waja volcanic sand via the coprecipitation method and to determine the effect of NaOH concentration on the resulting nanosilica characteristics, as well as the optimal synthesis conditions.

## Experimental Method

This research was conducted in four stages, namely: (1) preparation, (2) leaching, (3) synthesis, and (4) characterization.

**1. Preparation**

The volcanic sand samples were collected from the upstream area of Tukad Telaga Waja, Karangasem, Bali, which is one of the lahar pathways of Mount Agung. The samples were collected at depths of approximately 30–50 cm to minimize surface contamination.

The collected sand samples were repeatedly washed with distilled water until no visible dirt and suspended impurities remained, followed by drying in an oven at 100°C for 1 h. After drying, the sand was sieved through a 100-mesh sieve to achieve a more uniform particle-size distribution. Smaller particle domain sizes are known to improve leaching efficiency due to the increased reaction surface area [25].

Magnetic separation was subsequently performed manually using a permanent magnet several times to reduce ferromagnetic mineral impurities, particularly iron-containing particles, prior to chemical extraction. The prepared samples were then subjected to preliminary X-ray fluorescence (XRF) analysis to determine their oxide composition.

**2. Leaching Acid**

The leaching process was carried out using 3 M hydrochloric acid (HCl) to remove metal oxide impurities such as $Fe_2O_3$ and $Al_2O_3$ [26]. Acid treatment is known to effectively dissolve metal oxides while silica remains relatively stable under moderate acidic conditions [25,27]. The acid-leaching technique yielded 99% nanosilica purity using HCl, as reported by Mahmud et al. [28]. Therefore, acid leaching improves the removal of metallic impurities and increases the purity of the silica precursor prior to alkaline extraction.

Approximately 30 g of prepared sand was mixed with 240 mL of 3 M HCl (solid-liquid ratio 1: 8 w/v [29]. The suspension was heated to 80°C under continuous stirring for 2 hours to enhance the dissolution of metal oxide impurities while maintaining silica stability under acidic conditions. The dissolution reactions can be expressed as:

$$Fe_2O_3 + 6HCl \rightarrow 2FeCl_3 + 3H_2O \quad (1)$$
$$Al_2O_3 + 6HCl \rightarrow 2AlCl_3 + 3H_2O \quad (2)$$

Following leaching, the solution was filtered and washed with distilled water multiple times until the filtrate reached neutral pH (7) to remove residual chloride ions. The obtained solid residue was then dried at 100°C for 1 hour and used as a raw material for nanosilica synthesis.

**3. Synthesis**

Nanosilica was synthesized by coprecipitation. To ensure experimental consistency, all synthesis parameters, including temperature, stirring rate, reaction time, solid-to-liquid ratio, and drying conditions, were kept constant throughout the experiments, while only the NaOH concentration was varied. To minimize experimental variability, all synthesis procedures were conducted under identical experimental conditions for each NaOH concentration.

The acid-leached silica was dissolved in sodium hydroxide (NaOH) solution with concentrations of 6 M, 7M, and 8 M to investigate the effect of alkaline concentration on silica purity and structure.

Approximately 30 g of leached silica was reacted with 240 mL of NaOH solution at a solid-liquid ratio of 1:8 (w/v). The mixture was heated at 90°$C$ and stirred at 450 rpm for 2 hours to form a sodium silicate ($Na_2SiO_3$) solution. The dissolution reaction is given by:

$$SiO_2 + 2NaOH \rightarrow Na_2SiO_3 + H_2O \quad (3)$$

The resulting sodium silicate solution was filtered to remove insoluble residues. Coprecipitation was then carried out by titrating the sodium silicate solution dropwise with 2 M HCl until the pH decreased from the initial alkaline range of 13–14 to neutral (pH 7) [30]. Under these conditions, silica gel forms due to the polymerization of silanol groups [12,14].

The precipitation reactions are expressed as:

$$Na_2SiO_3 + 2HCl + H_2O \rightarrow Si(OH)_4 + 2NaCl \quad (4)$$

$$Si(OH)_4 \rightarrow SiO_2 + 2H_2O \quad (5)$$

The formed silica gel was aged for 36 hours at room temperature to allow the stabilization of the $Si - O - Si$ network [25]. The gel was then filtered, washed with distilled water to remove NaCl by-products, and the sample was dried in an oven at $100°C$ for 1 hour to obtain amorphous nanosilica powder [31].

**4. Characterization**

The synthesized nanosilica samples were characterized using an EDAX X-Ray Fluorescence (XRF) spectrometer operated at 30 kV and 1000 µA, with a measurement time of 150 s; X-Ray Diffraction (Bruker D8 Advance); and Scanning Electron Microscopy (Hitachi SU3500). XRD measurements were performed using Cu Kα radiation (λ = 1.54060 Å) operated at 40 kV and 40 mA in continuous PSD fast mode over a 2θ range of 10°–90° with a step size of 0.020° and a counting time of 0.10 s per step. The diffraction data were processed in Origin to determine the phase structure and to assess whether the synthesized $SiO_2$ was amorphous or crystalline [32]. XRF analysis was performed to determine the chemical composition and purity of the synthesized silica. Moreover, SEM analysis was conducted using a Hitachi SU3500 at an accelerating voltage of 15 kV, a magnification of 50,000×, and a working distance of 5.9 mm to observe the surface morphology, particle distribution, and agglomeration. Particle domain size was estimated from SEM micrographs using ImageJ software. Approximately 100 observable particle domains from each sample were manually measured, and the size distribution was analyzed using a log-normal distribution to estimate the average SEM-estimated particle domain size, acknowledging that the measured domains may represent agglomerated particles rather than individual primary nanoparticles.

The research workflow for synthesizing nanosilica with varying NaOH concentrations is depicted in Figure 1.

## Results and Discussion

The synthesis of $SiO_2$ nanoparticles from Tukad Telaga Waja volcanic sand using the coprecipitation method with NaOH concentrations of 6 M, 7 M, and 8 M was successfully carried out. As shown in Figure 1, the synthesis process produced white nanosilica powder for all concentrations. The formation of a white powder indicates the successful precipitation of silica compounds following alkaline extraction and acid neutralization.

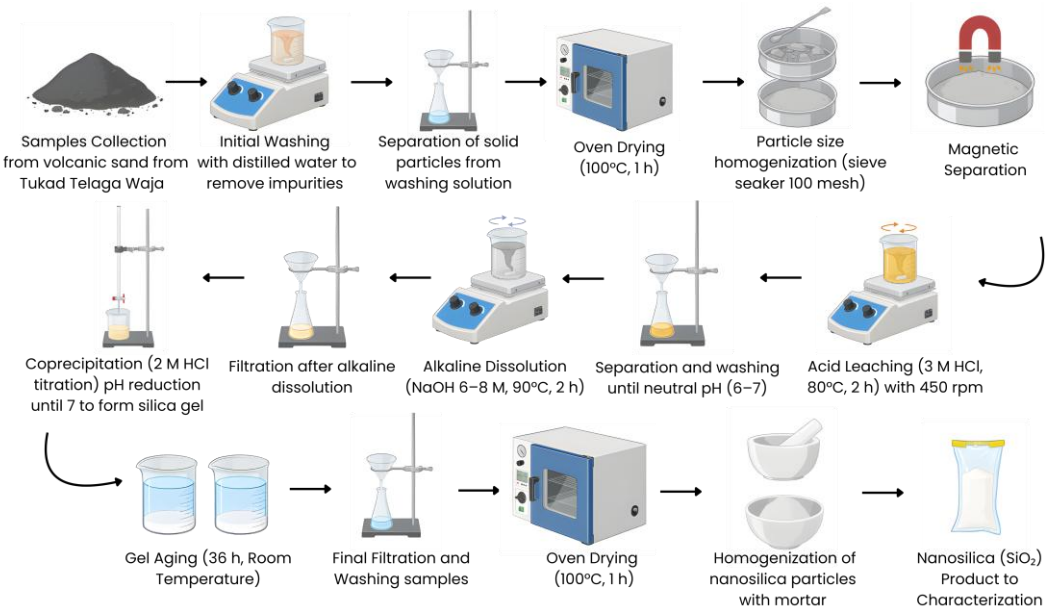


**Figure 1.** Flowchart of the Research Procedure

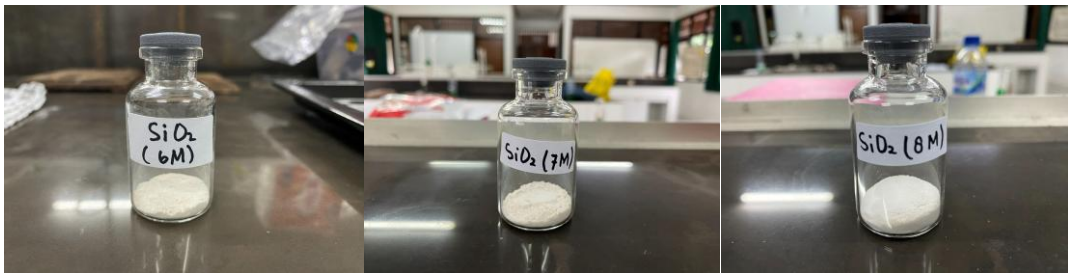


(a) (b) (c)

**Figure 2.** Nanosilica ($SiO_2$) powder obtained from the coprecipitation synthesis using Tukad Telaga Waja volcanic sand with NaOH concentrations of (a) 6 M, (b) 7 M, and (c) 8 M.

The mass yield of the synthesized nanosilica varied with the NaOH concentration used during extraction. The synthesis using 6 M NaOH produced 2.73% of nanosilica powder, whereas the 7 M NaOH treatment yielded 2.31%. The highest yield was obtained with 8 M NaOH, producing 3.69% of nanosilica powder. Although the yield did not increase monotonically with increasing NaOH concentration, the 8 M treatment resulted in the highest nanosilica recovery. The relatively lower yield obtained at 7 M may be attributed to variations in the precipitation efficiency or silica gel recovery during the washing and filtration steps. Overall, the results suggest that NaOH concentration influences silica extraction and precipitation efficiency, with 8 M providing the most favorable condition among the investigated concentrations.

The chemical composition of the raw volcanic sand and synthesized nanosilica was analyzed by X-ray fluorescence (XRF) to assess silica purity and impurity removal during synthesis. The XRF analysis of the raw material presented in Table 1 shows that the volcanic sand contains 42.2 wt% $SiO_2$ along with several impurity oxides, including $Fe_2O_3$, $Al_2O_3$, CaO, $TiO_2$, and MnO. The relatively high silica content indicates that Tukad Telaga Waja volcanic sand has strong potential as a natural precursor for nanosilica synthesis.

**Table 1.** Chemical composition of Tukad Telaga Waja volcanic sand based on XRF analysis

| Oxide | $SiO_2$ | $Fe_2O_3$ | $Al_2O_3$ | CaO | $TiO_2$ | MnO | Others |
|---|---|---|---|---|---|---|---|
| **(wt%)** | 42.2% | 26.2% | 13.0% | 14.0% | 1.94% | 0.47% | 0.17% |

After the coprecipitation synthesis, the $SiO_2$ content increased significantly across all NaOH concentrations. As shown in Table 2, the synthesized nanosilica obtained with 6 M NaOH exhibited a $SiO_2$ purity of 96.4 wt%, which increased to 97.7 wt% with 7 M NaOH and reached 98.9 wt% with 8 M NaOH. Compared with the initial silica content of the raw volcanic sand (42.2 wt%), the synthesis process successfully increased the silica purity by more than twofold while substantially reducing the concentration of impurity oxides.

The increase in $SiO_2$ purity is strongly influenced by the role of NaOH during the alkaline extraction stage. In the coprecipitation process, hydroxide ions ($OH^-$) from NaOH promote the dissolution of silica by breaking siloxane bonds (Si–O–Si) within the mineral structure, leading to the formation of soluble sodium silicate ($Na_2SiO_3$) [17-19]. Increasing NaOH concentration enhances the concentration of $OH^-$ ions, thereby improving silica dissolution efficiency and facilitating the separation of silica from impurity oxides such as $Fe_2O_3$, $Al_2O_3$, and CaO during the filtration stage [30]. As a result, a greater amount of dissolved silicate species becomes available for precipitation, producing nanosilica with higher purity. Similar results have also been reported by Meilani et al. [18] and Siswanto et al. [23], and Owoeye et al. [22] where increasing NaOH concentration improved silica extraction efficiency and increased the purity of synthesized nanosilica derived from natural silica sources.

**Table 2.** Chemical composition of volcanic sand after synthesis based on XRF analysis

| NaOH concentrations | $SiO_2$ | $Fe_2O_3$ | $K_2O$ | CaO | MnO | $TiO_2$ |
|---|---|---|---|---|---|---|
| **6 M** | 96.4 wt% | 1.6 wt% | 0.9 wt% | 0.8 wt% | 0.6 wt% | 0.2 wt% |
| **7 M** | 97.7 wt% | 0.7 wt% | 0.2 wt% | 0.7 wt% | 0.1 wt% | 0.4 wt% |
| **8 M** | 98.9 wt% | 0.4 wt% | 0.1 wt% | 0.3 wt% | 0.1 wt% | 0.2 wt% |

**Note**: *Oxides not listed in the table were not detected or were present below the detection limit of the XRF instrument.*

It should be noted that $Al_2O_3$, which was identified in the raw volcanic sand (Table 1), was not detected in the synthesized nanosilica samples by XRF. This suggests that the $Al_2O_3$ concentration decreased below the instrument detection limit after acid leaching and coprecipitation, indicating effective removal of aluminum-containing impurities.

Figure 3 presents the XRF spectra of the synthesized nanosilica for NaOH concentrations of 6 M, 7 M, and 8 M. The spectra show that the Si peak becomes increasingly dominant after the synthesis process, while the intensity of impurity-related peaks decreases significantly. This trend confirms that increasing NaOH concentration improves the extraction and purification efficiency of silica from the volcanic sand matrix.

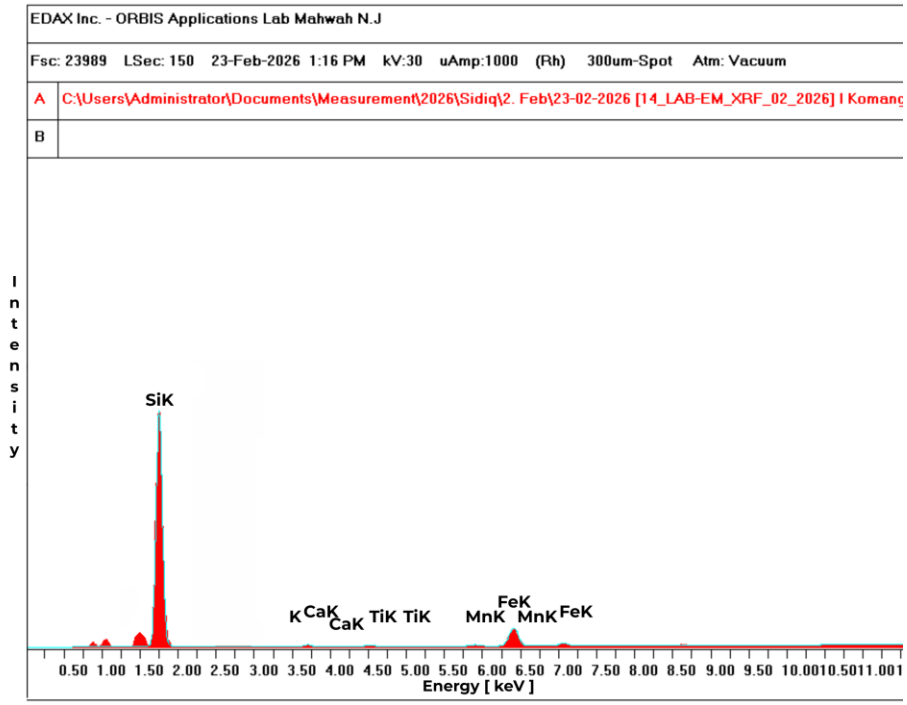
EDAX Inc. - ORBIS Applications Lab Mahwah N.J
Fsc: 23989 LSec: 150 23-Feb-2026 1:16 PM kV:30 uAmp:1000 (Rh) 300um-Spot Atm: Vacuum
A C:\Users\Administrator\Documents\Measurement\2026\Sidiq\2. Feb\23-02-2026 [14_LAB-EM_XRF_02_2026] I Komang
B
Intensity
SiK
K CaK CaK TiK TiK
FeK MnK MnK FeK
0.50 1.00 1.50 2.00 2.50 3.00 3.50 4.00 4.50 5.00 5.50 6.00 6.50 7.00 7.50 8.00 8.50 9.00 9.50 10.0010.5011.001
Energy [ keV ]

(a)

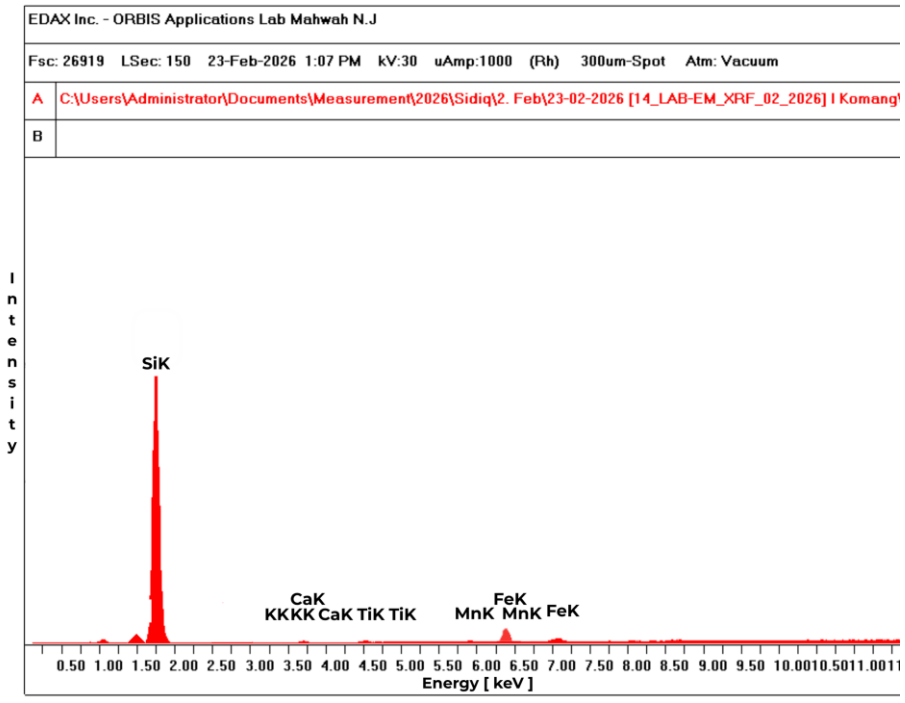
EDAX Inc. - ORBIS Applications Lab Mahwah N.J
Fsc: 26919 LSec: 150 23-Feb-2026 1:07 PM kV:30 uAmp:1000 (Rh) 300um-Spot Atm: Vacuum
A C:\Users\Administrator\Documents\Measurement\2026\Sidiq\2. Feb\23-02-2026 [14_LAB-EM_XRF_02_2026] I Komang
B
Intensity
SiK
CaK
K K K CaK TiK TiK
FeK
MnK MnK FeK
0.50 1.00 1.50 2.00 2.50 3.00 3.50 4.00 4.50 5.00 5.50 6.00 6.50 7.00 7.50 8.00 8.50 9.00 9.50 10.0010.5011.001
Energy [ keV ]

(b)

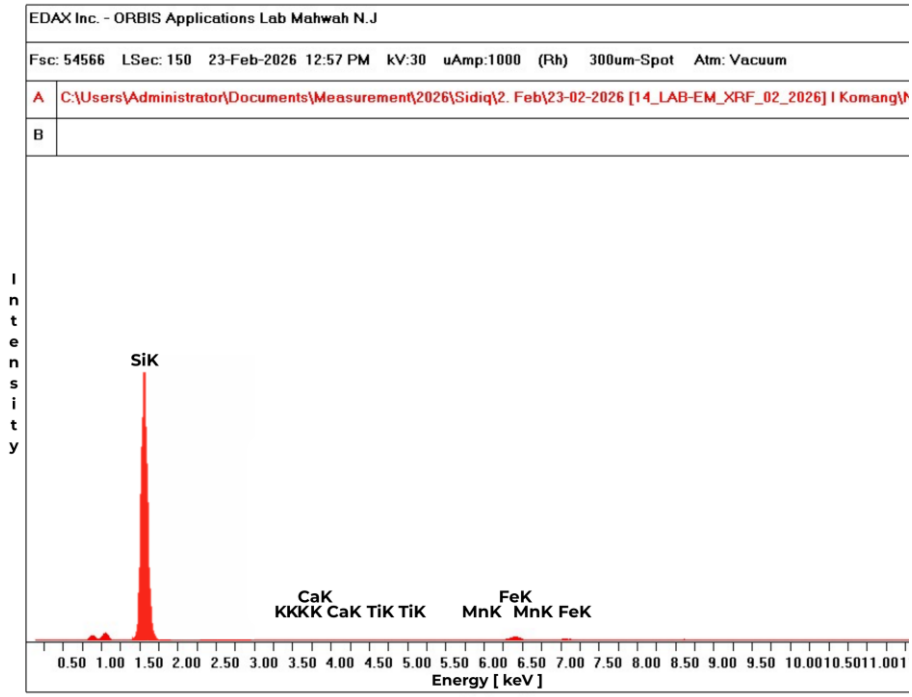


(c)

**Figure 3.** XRF spectra of synthesized $SiO_2$ nanoparticles with NaOH concentrations: (a) 6 M, (b) 7 M, and (c) 8 M.

The increasing dominance of the Si peak observed in the XRF spectra is consistent with the improved silica purity obtained from the quantitative XRF analysis. These findings further confirm that increasing NaOH concentration enhances silica extraction and impurity removal during the coprecipitation synthesis process [33,34].

The crystal structure of the synthesized $SiO_2$ nanoparticles was analyzed using X-Ray Diffraction (XRD) to identify the phase and structural characteristics of the synthesized material. The XRD diffraction patterns of the synthesized nanosilica prepared using NaOH molarity variations of 6 M, 7 M, and 8 M are presented in Figure 4.

The obtained diffraction patterns were also compared with the standard amorphous silica reference reported in the JCPDS database and in previous studies. Standard amorphous silica commonly exhibits a broad diffraction hump centered around $2\theta \approx 22°–24°$, which is associated with the absence of long-range crystalline ordering. In the present study, all synthesized samples exhibited a broad diffraction hump extending approximately from 20° to 30°, with the maximum intensity located near 23°–27°, indicating the predominance of an amorphous silica structure. This broad halo is consistent with the characteristic diffraction pattern of amorphous silica reported in standard databases and previous studies [17,26].

Although local intensity maxima were observed within the broad hump region, these features do not represent discrete crystalline diffraction peaks but rather intensity fluctuations commonly observed in amorphous materials. Therefore, they should not be interpreted as evidence of crystalline quartz. In contrast, crystalline silica phases such as quartz typically exhibit sharp diffraction peaks near 20.8°, 26.6°, 36.5°, and 50.1° according to ICDD PDF No. 46-1045. No sharp diffraction reflections corresponding to these crystalline phases were observed in the synthesized samples, confirming that the obtained $SiO_2$ remained predominantly amorphous.

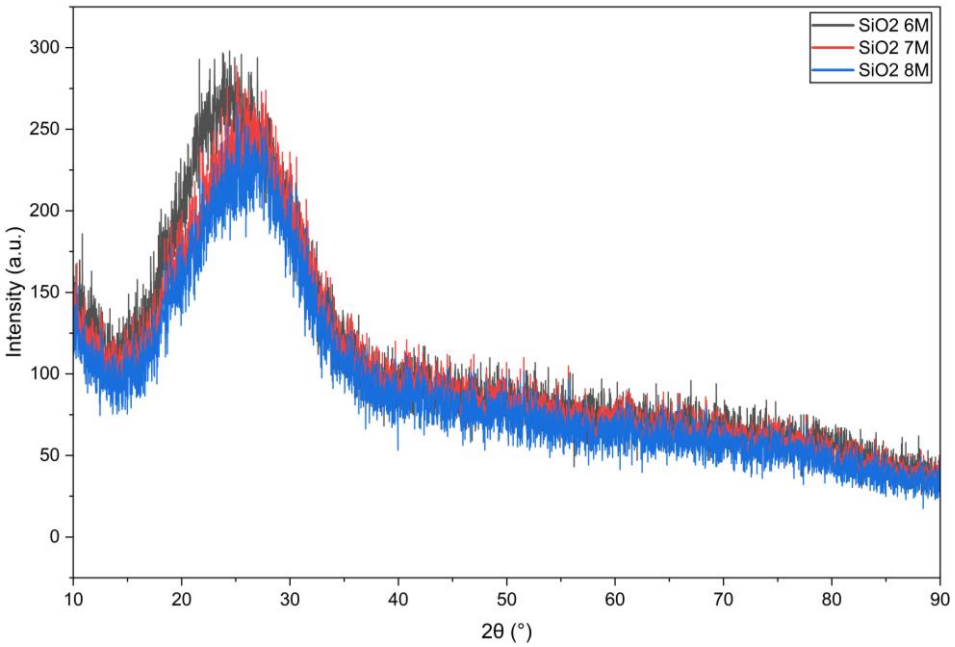


**Figure 4.** XRD diffraction pattern of $SiO_2$ nanoparticles under various conditions (6M, 7M, and 8M), which indicates an amorphous structure with a broad peak at 2θ ≈ 22-25°.

The formation of amorphous silica is closely related to the coprecipitation mechanism occurring during synthesis. During alkaline extraction, silica from the volcanic sand reacts with NaOH to form soluble sodium silicate ($Na_2SiO_3$). Subsequent acid neutralization promotes rapid hydrolysis and polycondensation, leading to the formation of silica gel networks with irregular atomic arrangements. The relatively fast precipitation and drying processes prevent the formation of an ordered crystalline lattice, leading to the formation of amorphous $SiO_2$ nanoparticles [22,35]. Although increasing the NaOH concentration enhanced silica extraction efficiency, it did not alter the silica's structural phase, as all samples consistently exhibited the characteristic broad amorphous diffraction hump.

Amorphous silica is generally preferred for various applications because its non-crystalline and irregular atomic structure provides higher surface reactivity compared with crystalline silica [36]. In addition, amorphous nanosilica typically possesses abundant silanol groups (Si–OH), a high surface area, and strong adsorption capacity, making it potentially suitable for applications such as adsorbents, catalyst supports, composite fillers, and surface modification materials. Furthermore, unlike crystalline silica, amorphous silica is considered safer for practical applications because it exhibits lower health risks associated with crystalline silica exposure [37].

The position and FWHM of the broad amorphous diffraction hump are summarized in Table 3 to describe the structural characteristics of the synthesized nanosilica.

**Table 3.** Characteristics of the amorphous diffraction hump obtained from XRD analysis

| Sample | Center of a broad hump ($2\theta$) | FWHM | Structural Interpretation |
|---|---|---|---|
| **6 M** | 23.82 | 1.40 | Amorphous |
| **7 M** | 25.78 | 1.05 | Amorphous |
| **8 M** | 25.99 | 1.40 | Amorphous |

The obtained results are consistent with previous studies. Silvia and Zainuri [17] reported that silica synthesized by the coprecipitation method exhibited a broad diffraction peak centered at 23° (2θ) that decreased gradually at higher angles. Similarly, Artha et al. [13] reported that nanosilica synthesized from volcanic materials using NaOH extraction also exhibited an amorphous diffraction pattern, characterized by a broad hump at 23°–24° (2θ). Therefore, the absence of sharp crystalline peaks in the present study confirms that the coprecipitation process successfully produced amorphous nanosilica from Tukad Telaga Waja volcanic sand.

To investigate the morphology and SEM-estimated particle domain size of the synthesized nanosilica, scanning electron microscopy (SEM) analysis was performed. The SEM micrographs of the synthesized $SiO_2$ nanoparticles prepared using NaOH concentrations of 6 M, 7 M, and 8 M are presented in Figure 5(a), (b), and (c), respectively.

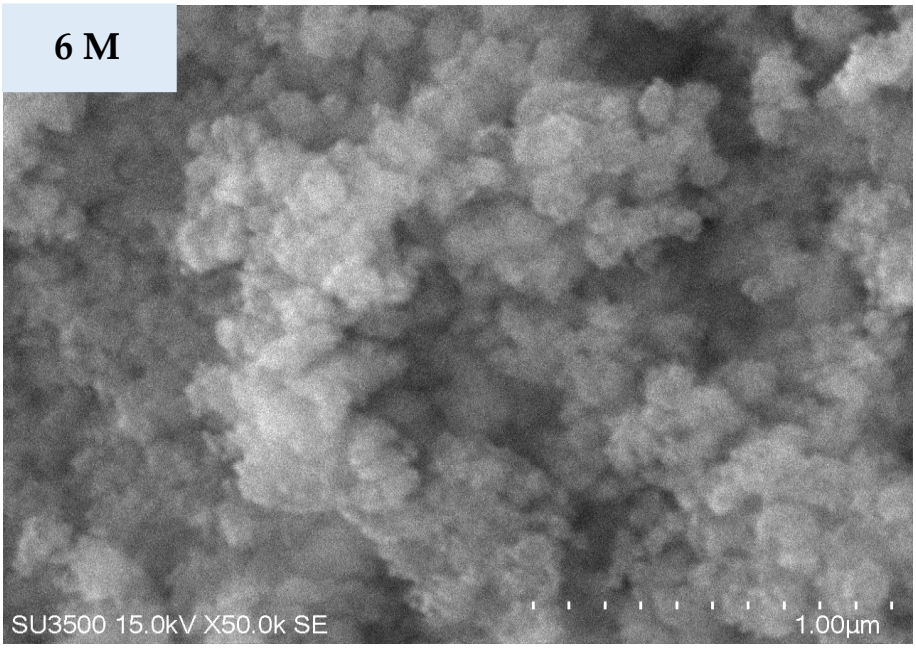


(a)

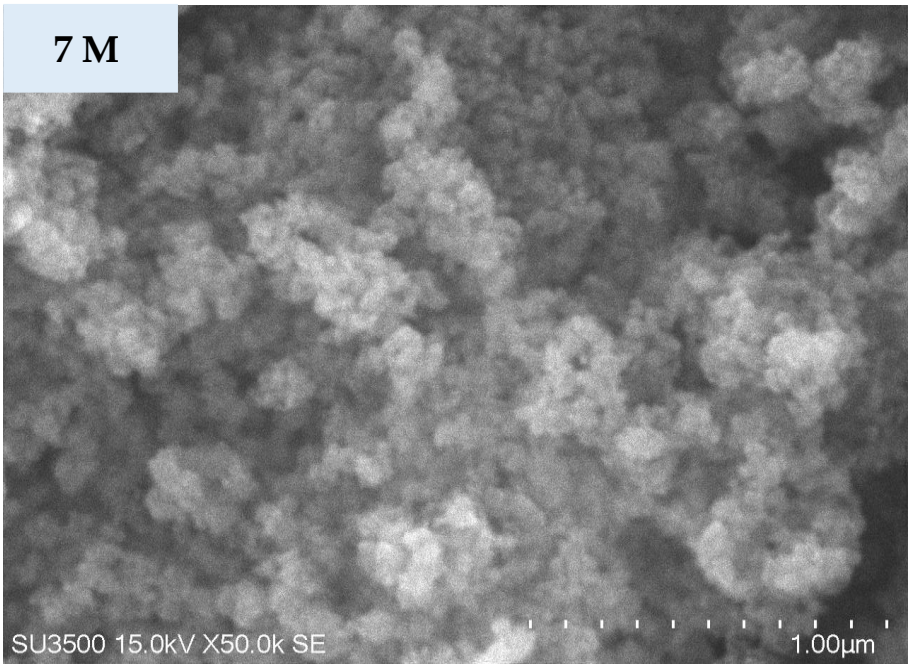


(b)

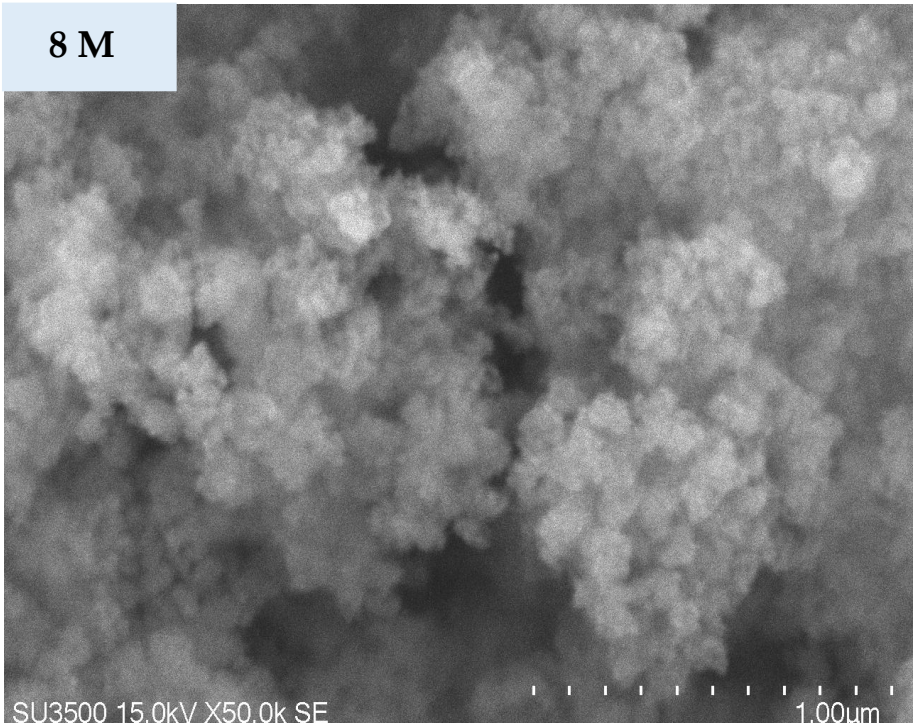


(c)

**Figure 5. S**EM images of synthesized $SiO_2$ nanoparticles obtained using NaOH concentrations of (a) 6 M, (b) 7 M, and (c) 8 M at a magnification of 50,000×.

As shown in Figure 5(a), the nanosilica synthesized using 6 M NaOH exhibits irregular granular morphology with agglomerated particle structures. Agglomeration is commonly observed in nanoparticle systems due to the high surface energy associated with nanoscale particles [38,39]. The particles appear relatively non-uniform and tend to form clustered aggregates. This phenomenon resulted in a non-uniform microstructure in the sample; however, it did not significantly affect the material's overall composition [40].

The SEM micrograph of the sample synthesized using 7 M NaOH, shown in Figure 5(b), still exhibits a granular, agglomerated morphology; however, the particle distribution appears relatively more homogeneous than that of the 6 M sample. This indicates that increasing the NaOH concentration influences the formation and distribution of silicate precursor species during coprecipitation, resulting in a more homogeneous particle morphology.

Meanwhile, the sample synthesized using 8 M NaOH (Figure 5(c)) exhibits finer particles with denser, more uniformly distributed agglomerates than those at lower concentrations. The formation of smaller particle domains at higher NaOH concentration is associated with increased silica dissolution and faster nucleation during the precipitation stage, leading to a greater number of nuclei and limiting excessive particle growth.

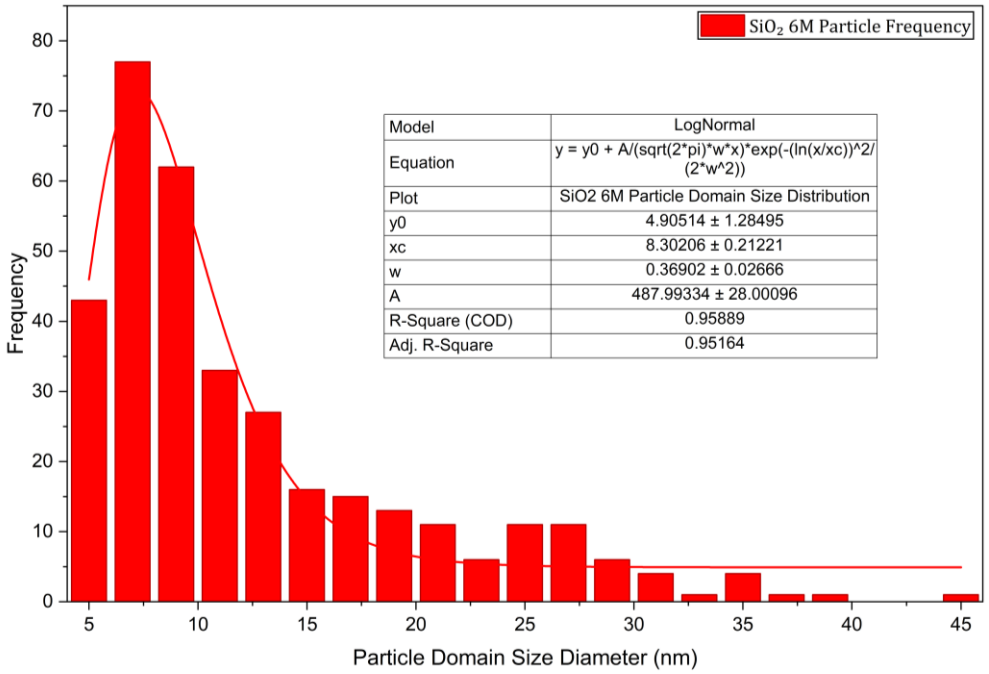
SiO2 6M Particle Frequency
Frequency
Particle Domain Size Diameter (nm)
Model LogNormal
Equation y = y0 + A/(sqrt(2*pi)*w*x)*exp(-(ln(x/xc))^2/(2*w^2))
Plot SiO2 6M Particle Domain Size Distribution
y0 4.90514 ± 1.28495
xc 8.30206 ± 0.21221
w 0.36902 ± 0.02666
A 487.99334 ± 28.00096
R-Square (COD) 0.95889
Adj. R-Square 0.95164

(a)

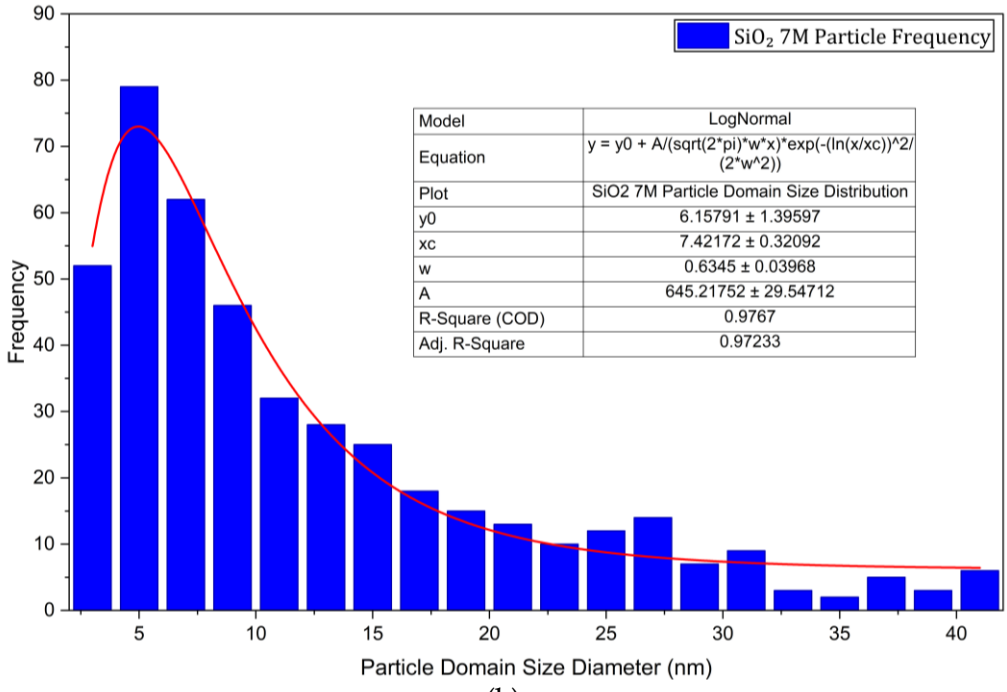
SiO2 7M Particle Frequency
Frequency
Particle Domain Size Diameter (nm)
Model LogNormal
Equation y = y0 + A/(sqrt(2*pi)*w*x)*exp(-(ln(x/xc))^2/(2*w^2))
Plot SiO2 7M Particle Domain Size Distribution
y0 6.15791 ± 1.39597
xc 7.42172 ± 0.32092
w 0.6345 ± 0.03968
A 645.21752 ± 29.54712
R-Square (COD) 0.9767
Adj. R-Square 0.97233

(b)

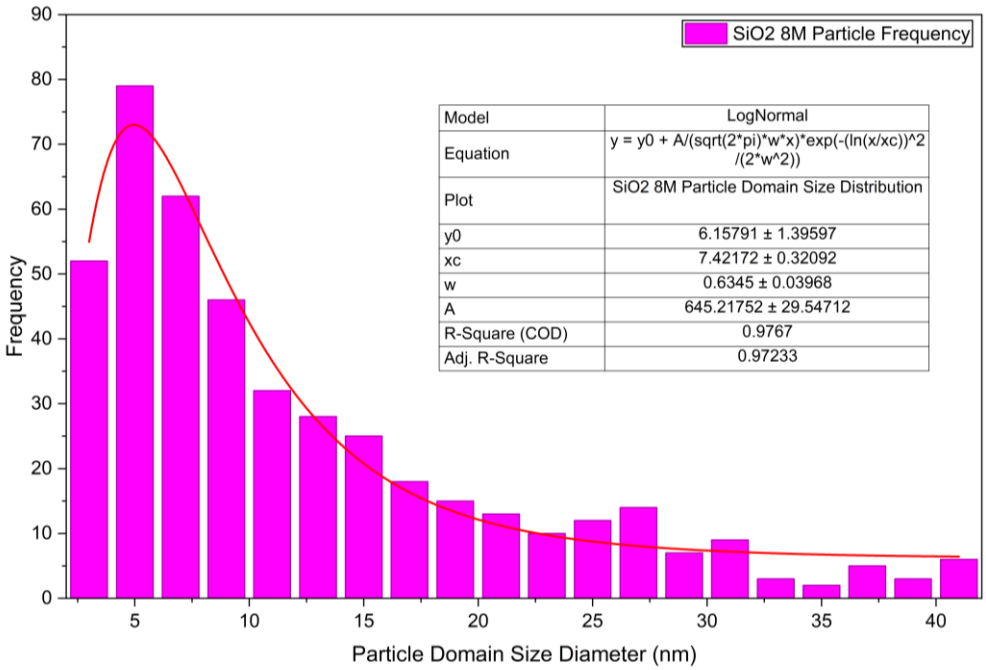


(c)

**Figure 6.** SEM-estimated particle domain size distribution histograms and corresponding log-normal fitting curves of synthesized $SiO_2$ obtained from ImageJ analysis for NaOH concentrations of (a) 6 M, (b) 7 M, and (c) 8 M.

Particle domain size was estimated from SEM micrographs using ImageJ, with approximately 100 particle domains per sample measured. Owing to the agglomerated morphology of the synthesized nanosilica, the measured dimensions represent SEM-estimated particle domain sizes rather than the actual primary nanoparticle size. The obtained domain size distributions were evaluated using a log-normal fitting approach to estimate the characteristic domain size. The histogram distributions shown in Figure 6 indicate that most observable particle domains fall within the nanoscale range, although larger agglomerated domains are also present. The fitted curves exhibit good agreement with the experimental data, as indicated by the relatively high coefficient of determination ($R^2$) values.

**Table 4.** Log-normal fitting parameters and SEM-estimated average particle domain size of synthesized $SiO_2$

| Sample | Xc (nm) | w | $R^2$ | Average particle domain size (nm) |
|---|---|---|---|---|
| **$SiO_2$ 6 M** | 8.30206 ± 0.21221 | 0.36902 ± 0.02666 | 0.95889 | 8.3 |
| **$SiO_2$ 7 M** | 7.42172 ± 0.32092 | 0.6345 ± 0.03968 | 0.9767 | 7.4 |
| **$SiO_2$ 8 M** | 6.04679 ± 0.34174 | 0.58828 ± 0.06045 | 0.95807 | 6.0 |

Based on the log-normal fitting analysis summarized in Table 4, the SEM-estimated characteristic particle domain size decreased with increasing NaOH concentration. The synthesized nanosilica prepared using 6 M NaOH exhibited an estimated average particle domain size of 8.30 nm, which decreased to 7.42 nm for the 7 M sample and further to 6.05 nm for the 8 M sample. Although these values should not be interpreted as the actual primary nanoparticle size, they suggest that increasing the NaOH concentration alters particle formation behavior during coprecipitation, leading to finer observable particle domains. The reduction in the estimated domain size is also associated with the increased

hydroxide ion ($OH^-$) concentration during alkaline extraction, which promotes silica dissolution and enhances nucleation during precipitation.

In addition, the estimated particle domain size distribution histograms presented in Figure 6(a)–(c) indicate that the particle populations follow a log-normal distribution, which is commonly observed in nanoparticle synthesis processes involving nucleation and particle growth mechanisms. The relatively high coefficient of determination ($R^2$) values obtained from the fitting analysis indicate good agreement between the experimental data and the log-normal model. However, the particle domain sizes obtained from SEM-ImageJ analysis should be regarded as approximate estimates, as the synthesized nanosilica exhibits a highly agglomerated morphology, making the boundaries of individual primary nanoparticles difficult to distinguish. Furthermore, SEM observations at 50,000× magnification have limited capability to accurately resolve primary particles below approximately 10 nm. Consequently, the measured values more appropriately represent observable particle domains or agglomerates rather than the actual primary nanoparticle size. Therefore, complementary characterization techniques, such as Transmission Electron Microscopy (TEM) or Dynamic Light Scattering (DLS), are recommended to accurately verify nanoscale particle size and morphology.

Although SEM-ImageJ analysis suggests that the observable particle domains are within the nanoscale range, these values should be interpreted only as SEM-estimated particle domain sizes rather than definitive primary nanoparticle dimensions. Nevertheless, the consistent reduction in the estimated particle domain size with increasing NaOH concentration indicates that variations in NaOH concentration influence particle formation behavior during coprecipitation while maintaining the amorphous structure of the synthesized $SiO_2$.

In this study, NaOH concentration was found to play a dominant role in determining the physicochemical characteristics of the synthesized nanosilica compared with other synthesis parameters such as temperature and reaction time. The alkaline environment generated by NaOH directly controls the cleavage of Si–O–Si bonds within the silica structure, thereby governing the dissolution efficiency of silica from volcanic sand precursors [41,42]. This observation is consistent with the study reported by Raditya et al. [20], which demonstrated that NaOH concentration has a stronger influence on silica precipitation and purity than reaction temperature or extraction time. In the present work, increasing the NaOH concentrations from 6 M to 8 M significantly improved the $SiO_2$ purity from 96.4 wt% to 98.9 wt%, indicating that higher hydroxide ion ($OH^-$) concentration enhances the formation of soluble sodium silicate ($Na_2SiO_3$) during alkaline extraction.

The effectiveness of this dissolution process is also closely related to the initial silica structure in volcanic sand. Volcanic silica generally exists in amorphous or semi-crystalline phases, which possess higher chemical reactivity than crystalline silica due to their disordered atomic arrangement [11]. Consequently, increasing NaOH concentration accelerates silica dissolution and increases the concentration of dissolved silicate precursors available during the coprecipitation stage.

The increased concentration of dissolved silicate species subsequently affects the nucleation mechanism during precipitation. Higher supersaturation conditions promote rapid nucleation, leading to more nuclei formed in a shorter time [43]. Because the available precursor is distributed among many nuclei simultaneously, particle-domain growth is more limited, leading to smaller nanosilica particle domains. This mechanism explains the

observed reduction in average particle domain size from 8.30 nm at 6 M NaOH to 6.05 nm at 8 M NaOH. Therefore, the decrease in particle domain size is not merely a morphological observation but is strongly associated with the increase in nucleation rate induced by higher alkaline concentration.

However, the formation of smaller particle domains also increases surface energy, making nanoparticles thermodynamically unstable and more prone to agglomeration. This behavior is evident in the SEM micrographs, where the 8 M sample shows denser agglomeration than the 6 M sample. Despite this agglomeration phenomenon, XRD analysis confirms that all synthesized samples remain in the amorphous phase. The absence of sharp crystalline peaks indicates that the coprecipitation process occurs rapidly, preventing long-range atomic ordering and crystalline growth. Amorphous silica is advantageous because its disordered structure provides higher reactivity and a larger accessible surface area compared with crystalline silica [35,36].

The amorphous structure and relatively small SEM-estimated particle domain size obtained in this study suggest that the synthesized nanosilica may provide favorable characteristics for future functional applications. Although the present study did not include BET surface area analysis, FTIR characterization, or application performance tests, amorphous nanosilica is generally reported to possess abundant surface silanol (Si–OH) and siloxane (Si–O–Si) groups that contribute to adsorption and surface interaction processes [44,45]. Therefore, the synthesized nanosilica may be further explored for potential applications as an adsorbent for heavy metal and dye removal in wastewater treatment, as a catalyst support material, and as a reinforcing filler in composite systems [37,46,47]. In addition, the use of volcanic sand as a local silica source demonstrates the potential for developing low-cost, sustainable nanosilica production using abundant natural resources [48].

These findings also provide an important basis for future studies. Since NaOH concentration strongly influences silica dissolution, nucleation behavior, particle domain size, and product purity, further optimization across broader NaOH concentration ranges, precipitation conditions, and complementary characterization techniques such as TEM, BET, and FTIR would be valuable for a more comprehensive understanding of nanosilica formation mechanisms and surface properties. Although FTIR analysis was not conducted in the present study due to limited instrument availability, the functional groups commonly associated with amorphous silica, including siloxane (Si–O–Si) and silanol (Si–OH), should be verified by FTIR in future studies.

## Conclusion

The synthesis of $SiO_2$ nanoparticles from Tukad Telaga Waja volcanic sand was successfully carried out using the coprecipitation method with NaOH concentrations of 6 M, 7 M, and 8 M. The results demonstrate that NaOH concentration plays an important role in controlling the physicochemical characteristics of the synthesized nanosilica. Increasing NaOH concentration enhanced silica dissolution efficiency during alkaline extraction, resulting in higher $SiO_2$ purity and smaller SEM-estimated particle domain size while maintaining the amorphous structure of the synthesized material. Among the investigated conditions, 8 M NaOH produced the optimum physicochemical characteristics with the highest silica purity and the SEM-estimated particle domain size. XRD analysis confirmed that all synthesized samples exhibited an amorphous structure, characterized by a broad diffraction hump around $2\theta \approx 23$ °- 27 °, while SEM analysis revealed irregular granular morphology with a tendency toward agglomeration. These

findings indicate that volcanic sand from Tukad Telaga Waja has strong potential as a sustainable local precursor for the production of high-purity nanosilica. Furthermore, the synthesized nanosilica may be further explored for potential applications such as adsorbents, catalyst supports, and functional composite fillers. However, this study remains limited in its characterization of primer particle size, as it relies solely on SEM analysis. Therefore, further studies using complementary characterization techniques, such as TEM, FTIR, and BET, are recommended to provide a more comprehensive evaluation of nanosilica properties and formation mechanisms.

## Acknowledgment

The authors would like to extend their most sincere appreciation to the lecturers of the Physics Study Program at Universitas Pendidikan Ganesha for their invaluable advice and guidance in conducting the research. The authors would also like to extend their gratitude to Pusat Penelitian Nanosains dan Nanoteknologi (PPNN), located at Institut Teknologi Bandung, for their invaluable assistance in conducting the material characterization. Furthermore, the authors would like to extend their appreciation to the local government of Tukad Telaga Waja, Karangasem, Bali, for their assistance in conducting the sampling.

## References

[1] N. I. Mohamed, "Quantification of silicon (Si) and silicon dioxide ($SiO_2$) from the Nafud Desert-Al-Qassim region, Kingdom of Saudi Arabia using XRD analysis," *Advances in Materials Physics and Chemistry*, vol. 14, no. 05, pp. 67–75, 2024.

[2] A. Luthfiah, Y. Deawati, M. L. Firdaus, I. Rahayu, and D. Rakhmawaty Eddy, "Silica from natural sources: A review on the extraction and potential application as a supporting photocatalytic material for antibacterial activity," 2021.

[3] A. B. Prasetyo *et al.*, "Development of high purity amorphous silica from emulsifier silicon by pyrolysis process at a temperature of 700 °C," *J. Phys. Conf. Ser.*, vol. 2190, no. 1, p. 012013, Mar. 2022.

[4] R. E. Kirk and D. F. Othmer, *Kirk-Othmer Encyclopedia of Chemical Technology*. Wiley, 2000.

[5] I. Khan, K. Saeed, and I. Khan, "Nanoparticles: Properties, applications and toxicities," *Arabian Journal of Chemistry*, vol. 12, no. 7, pp. 908–931, Nov. 2019.

[6] L. A. Kolahalam, I. V. Kasi Viswanath, B. S. Diwakar, B. Govindh, V. Reddy, and Y. L. N. Murthy, "Review on nanomaterials: synthesis and applications," *Mater. Today, Proc.*, vol. 18, pp. 2182–2190.

[7] P. Agus Prayogi, I. Putu, and T. Raditya, "Autentisitas sungai telaga waja dalam pengembangan pariwisata berkelanjutan di kabupaten karangasem," *Journal of Tourism and Interdisciplinary Studies (JoTIS)*, vol. 5, no. 2, pp. 453–465, Dec. 2025.

[8] A. Setyo Pratomo, Y. Prasetyo, and S. Subiyanto, "Analisis deformasi dan pemetaan potensi dampak aliran lava pada kawasan Gunung Agung," *Jurnal Geodesi Undip*, vol. 7, no. 4, pp. 119–127, Dec. 2018.

[9] N. P. S. N. Utari, I. W. Sudiarta, and P. Suarya, "Sintesis dan karakterisasi silika gel dari abu vulkanik Gunung Agung melalui teknik sol-gel," *Jurnal Kimia*, vol. 14, no. 1, pp. 30–36, Feb. 2020.

[10] M. Nanzyo, "Unique properties of volcanic ash soils," *Global Environmental Research*, vol. 6, no. 2, pp. 99–112, 2002.

[11] Astari, A. P. Hendrawan, and E. Yuliani, "Evaluasi karakteristik mikro-fisik dan mekanik pasir vulkanik tersementasi di tebing sungai aliran lahar gunung kelud," *Jurnal Teknologi dan Rekayasa Sumber Daya Air*, vol. Vol.1 No.2, pp. 661–671, 2021, Accessed: Dec. 25, 2025.

[12] L. Yogantari dan Sulistyani, "Purifikasi silika dari pasir vulkanik Gunung Merapi sebagai bahan baku sel fotovoltaik," *Jurnal Elemen Kimia*, vol. 5, no. 3, 2016.

[13] I. K. R. W. Artha, I. B. P. Mardana, and G. Arjana, "Synthesis and characterization of nanosilica ($SiO_2$) volcanic rock of Mount Batur in Bali," *Indonesian Physical Review*, vol. 7, no. 2, pp. 268–280, 2024.

[14] M. Hasanah *et al.*, "Extraction of silica dioxide ($SiO_2$) from Mount Sinabung volcanic ash with the coprecipitation method," *IOP Conf. Ser. Mater. Sci. Eng.*, vol. 1156, no. 1, p. 012015, Jun. 2021.

[15] E. Katoueizadeh, M. Rasouli, and S. M. Zebarjad, "A comprehensive study on the gelation process of silica gels from sodium silicate," *Journal of Materials Research and Technology*, vol. 9, no. 5, pp. 10157–10165, Sep. 2020.

[16] I. Ramadhani, B. Oktavia, A. Putra, and H. Sanjaya, "Penentuan kondisi optimum pembentukan natrium silikat ($Na_2SiO_3$) menggunakan material dasar silika alam dan natrium hidroksida (NaOH)," *PERIODIC: Chemistry Journal of Universitas Negeri Padang*, vol. 10, no. 2, 2021.

[17] L. Silvia and M. Zainuri, "Analisis silika ($SiO_2$) hasil kopresipitasi berbasis bahan alam menggunakan uji XRF dan XRD," *Jurnal Fisika dan Aplikasinya*, vol. 16, no. 1, pp. 12–17, Feb. 2020.

[18] B. Dwi Meilani *et al.*, "Synthesis of red mud-based $SiO_2$ with various NaOH concentration and extraction times," *Indonesian Journal of Chemical Science*, vol. 12, no. 3, pp. 305–316, 2023.

[19] S. H. Ghasemzadeh Mousavinejad and M. Sammak, "An assessment of the effect of $Na_2SiO_3$/NaOH ratio, NaOH solution concentration, and aging on the fracture properties of ultra-high-performance geopolymer concrete: The application of the work of fracture and size effect methods," *Structures*, vol. 39, pp. 434–443, May 2022.

[20] R. Raditya Ginanjar, A. Ma'ruf, and A. H. Mulyadi, "Ekstraksi silika dari abu sekam padi menggunakan pelarut NaOH," in *Prosiding Seminar Nasional Hasil*, Purwokerto: Semantic Scholar, Dec. 2014, pp. 306–312. Accessed: Apr. 24, 2026.

[21] A. Ismayana, A. Maddu, I. Saillah, E. Mafquh, and N. Siswi Indrasti, "Sintesis nanosilika dari abu ketel industri gula dengan metode ultrasonikasi dan penambahan surfaktan," *Jurnal Teknologi Industri Pertanian*, vol. 27, no. 2, pp. 228–234, Nov. 2017.

[22] S. S. Owoeye, S. M. Abegunde, and B. Oji, "Effects of process variable on synthesis and characterization of amorphous silica nanoparticles using sodium silicate solutions as precursor by sol–gel method," *Nano-Structures and Nano-Objects*, vol. 25, Feb. 2021.

[23] Siswanto, A. Supardi, and A. Nurhaeni, "Synthesis of amorphous silica ($SiO_2$) from natural sand minerals using the precipitation method," in *THE 7th INTERNATIONAL CONFERENCE ON SCIENCE AND APPLIED SCIENCE (ICSAS 2022)*, 2024, p. 070010.

[24] N. I. Ramadhan, Munasir, and Triwikantoro, "Sintesis dan karakterisasi serbuk $SiO_2$ dengan variasi ph dan molaritas berbahan dasar pasir bancar, Tuban," *Jurnal Sains dan Seni Pomits*, vol. 3, no. 1, pp. 2337–3520, 2014.

[25] R. K. Iler, *The chemistry of silica: solubility, polymerization, colloid and surface properties, and biochemistry*. Wiley, 1979. Accessed: Apr. 20, 2026. [Online]. Available: https://books.google.co.id/books?id=Dc0RAQAAIAAJ.

[26] I. Abdellaoui, M. M., Islam, T., Sakurai, S., Hamzaoui, and K. Akimoto, "Impurities removal process for high-purity silica production from diatomite," *Hydrometallurgy*, vol. 179, pp. 207–214, Aug. 2018.

[27] T. Zhong, W. Yu, C. Shen, and X. Wu, "Research on preparation and characterization of high-purity silica sands by purification of quartz vein ore from Dabie Mountain," *Silicon*, vol. 14, no. 9, pp. 4723–4729, Jun. 2022.

[28] A. Mahmud, P. S. M. Megat-Yusoff, F. Ahmad, and A. A. Farezzuan, "Acid leaching as efficient chemical treatment for rice husk in production of amorphous silica nanoparticles," vol. 11, no. 22, pp. 13384–13388, 2016, [Online]. Available: www.arpnjournals.com

[29] D. Kong, Y. Gao, S. Song, and R. Jiang, "Kinetics and mechanism of $SiO_2$ extraction from acid-leached coal gangue residue by alkaline hydrothermal treatment," *Materials*, vol. 17, no. 17, Sep. 2024.

[30] S. Silahooy, "Analisis serbuk silika amorf ($SiO_2$) berbahan dasar pasir," *Scie Map J*, vol. 2, no. 2, pp. 75–78, 2020, Accessed: Apr. 04, 2026. [Online]. Available: https://ojs3.unpatti.ac.id/index.php/sciencemap/article/view/3818.

[31] D. Mart Shoodiqin, F. Robiandi, R. Cahya Chairunnisa, D. M. Shoodiqin, F. Robiandi, and R. C. Chairunnisa, "Synthesis of nano-silica from loa kulu rice husk using the sol-gel method," *Indonesian Physical Review*, vol. 7, no. 1, pp. 125–132, 2024.

[32] X. Ke *et al.*, "A rapid analytical method for the specific surface area of amorphous $SiO_2$ based on X-Ray diffraction," *J. Non. Cryst. Solids*, vol. 531, Mar. 2020.

[33] S. N. Ishmah, M. D. Permana, M. L. Firdaus, and D. R. Eddy, "Extraction of silica from Bengkulu beach sand using alkali fusion method," PENDIPA Journal of Science Education, vol. 4, no. 2, pp. 1–5, Jun. 2020.

[34] D. Nggolaon, S. Silahooy, G. W. Jaya, and N. Hattu, "Analisis dan karakterisasi senyawa silika ($SiO_2$) berbahan dasar batuan vulkanik di Pulau Ambon," *Jurnal Kumparan Fisika*, vol. 7, no. 3, pp. 98–105, Dec. 2024.

[35] M. D. Utama *et al.*, "Synthesis and application of sol-gel-derived nano-silica in glass ionomer cement for dental cementation," *Biomimetics*, vol. 10, no. 4, pp. 235–247, Apr. 2025.

[36] Risfaheri *et al.*, "Sustainable production of high-purity amorphous silica from rice husk: A comparative study on the impact of fresh and reused hydrochloric acid leaching," *S. Afr. J. Chem. Eng.*, vol. 56, Apr. 2026.

[37] Z. Ezzeddine, I. Batonneau-Gener, G. Ghssein, and Y. Pouilloux, "Recent advances in heavy metal adsorption via organically modified mesoporous silica: A review," Mar. 01, 2025, *Multidisciplinary Digital Publishing Institute (MDPI)*.

[38] H. Susilo and A. Putra, "Pengaruh konsentrasi naoh pada sintesis nanosilika dari sinter silika mata air panas Sentral, Solok Selatan, Sumatera Barat dengan metode kopresipitasi," *Jurnal Fisika Unand*, vol. 5, no. 4, pp. 334–338, 2016.

[39] A. H. Daulay, Masthura, and A. Pratiwi, "Analisis pengaruh variasi suhu pembakaran terhadap mikrostruktur dan kandungan silika abu kulit kakao (theobroma cacao) dengan metode SEM dan XRD," *JFT: Jurnal Fisika dan Terapannya*, vol. 9, no. 2, pp. 89–98, Dec. 2022.

[40] H. Kiswanto, "Analisis perubahan struktur kristal dan distribusi kation cobalt ferrite akibat substitusi zinc," *Jurnal Ilmu dan Inovasi Fisika*, vol. 4, no. 2, pp. 155–163, Aug. 2020.

[41] F. Adam, T. S. Chew, and J. Andas, "A simple template-free sol-gel synthesis of spherical nanosilica from agricultural biomass," *J. Sol-Gel Sci. Technol.*, vol. 59, no. 3, pp. 580–583, Sep. 2011.

[42] K. V Selvakumar, A. Umesh, P. Ezhilkumar, S. Gayatri, P. Vinith, and V. Vignesh, "Extraction of silica from burnt paddy husk," *Recent Trends in Biotechnology and Chemical Engineering*, vol. 6, no. 9, pp. 4455–4459, 2014, Accessed: May 12, 2026. [Online]. Available: https://sphinxsai.com/2014/RTBCE/6/(4455-4459)%20014.pdf

[43] N. A. M. Syafira and A. Priyono, "Studi literatur: Perkembangan nanomaterial," *BERKALA FISIKA*, vol. 25, no. 3, pp. 111–121, 2022, Accessed: May 14, 2026. [Online]. Available:https://ejournal.undip.ac.id/index.php/berkala_fisika/article/view/50741/22684

[44] S. Zhao, Z. Ji, C. Wang, and J. Du, "Synthesis of mesoporous $SiO_2$ glass by a novel chemical method," *Mater. Lett.*, vol. 61, no. 3, pp. 897–899, Feb. 2022.

[45] I. S. Hardyanti, I. Nurani, D. S. Hardjono HP, E. Apriliani, and E. A. P. Wibowo, "Pemanfaatan silika ($SiO_2$) dan bentonit sebagai adsorben logam berat Fe pada limbah batik," *JST (Jurnal Sains Terapan)*, vol. 3, no. 2, Oct. 2017.

[46] M. Shalit, Y. Knop, M. Radune, and Y. Mastai, "Innovative application of standard sand as a functional carrier for nano-silica in cement," *Materials*, vol. 18, no. 18, Sep. 2025.

[47] R. Fatima, P. Katiyar, and K. Kushwaha, "Recent advances in mesoporous silica nanoparticle: Synthesis, drug loading, release mechanisms, and diverse applications," *Frontiers in Nanotechnology*, vol. 7, 2025.

[48] N. Baig, I. Kammakam, W. Falath, and I. Kammakam, "Nanomaterials: A review of synthesis methods, properties, recent progress, and challenges," Mar. 21, 2021, *Royal Society of Chemistry*.